Bull. Chem. Soc. Ethiop. **2013**, 27(1), 49-56. ISSN 1011-3924
Printed in Ethiopia
DOI: http://dx.doi.org/10.4314/bcse.v27i1.5

SYNTHESIS OF M–Nd DOPED Fe_3O_4 NANOPARTICLES (M = Co, Ce, Cr, Ni) WITH TUNABLE MAGNETIC PROPERTIES

Mohammad Yousefi* and Paransa Alimard

Department of Chemistry, Shahr-e-Rey Branch, Islamic Azad University, Tehran, Iran

(Received May 17, 2011; revised November 22, 2012)

ABSTRACT. Magnetic nanoparticles were prepared by the aqueous co-precipitation method. The magnetic nanoparticles obtained were characterized systematically through the use of an X-ray diffraction (XRD), energy dispersive X-ray spectroscopy (EDS), scanning electron microscope (SEM), transmission electron microscope (TEM), Fourier transform infrared spectroscopy (FT-IR) and a vibrating sampling magnetometer (VSM). The results revealed that the magnetic nanoparticles were spherical shaped with inverse spinel structure. The size of Fe_3O_4 and Nd-Co doped Fe_3O_4 magnetic nanoparticles were approximately 15 nm. Magnetic measurement revealed that the nanoparticles were super paramagnetic at room temperature. It was found that the magnetic response of the Fe_3O_4 increased when it was doped with Nd^{3+} and Co^{2+}. However, the magnetic response of the Fe_3O_4 decreased when it was doped with Nd^{3+} or Ce^{3+} or Cr^{3+}or Ni^{2+}.

KEYWORDS: Fe_3O_4, Magnetic nanoparticles, Superparamagnetic, Magnetite, Fe_3O_4 doped

INTRODUCTION

Nanoparticles (NPs) have been a topic of intense research mainly because of their unique physical and chemical properties compared to their bulky counterparts. The case of magnetic NPs is especially interesting since the NP size is comparable to that of a magnetic domain that results in the unusual magnetic phenomena of superparamagnetism [1]. Magnetite (Fe_3O_4) is a common spinel ferrite containing a cubic inverse spinel structure. Oxygen forms a FCC closed packing and Fe cations occupying the interstitial tetrahedral sites and octahedral sites [2]. The electrons can hop between Fe^{2+} and Fe^{3+} ions in the octahedral sites at room temperature, rendering magnetite an important part of half-metallic materials. The development of uniform spinel ferrite nanocrystals has been intensively pursued in the applications of ferrofluids [3], catalysis [4], biomedical applications such as magnetic resonance imaging (MRI) [5], drug targeting [6-7] and hyperthermia [8], data storage [9], microwave absorption [10] and magnetorheological fluids [11, 12]. Many reports proved that the property of spinel ferrites can be improved by doping metal elements in MFe_2O_4 owing to their enhanced crystal anisotropy [13]. To obtain nano sized spinel ferrite particles, various preparation techniques have been developed. Some of these preparation approaches are hydrothermal synthesis [14-19], co-precipitation [20-22], sol-gel [23, 24] and microemulsion processes [25-29]. In this work, a new series of Nd, Nd-Co, Nd-Ce, Nd-Cr, Nd-Ni doped Fe_3O_4 nanoparticles were successfully synthesized by co-precipitation method. All the reagents were cheap inorganic materials. Also, no surfactants were used in the system. In this investigation, the as-prepared composite NPs had good crystal structure, small particle size and high magnetic saturation.

*Corresponding author. E-mail: myousefi50@yahoo.com

EXPERIMENTAL

Material and methods

Ferrous sulfate ($FeSO_4 \cdot 7H_2O$), anhydrous ferric chloride ($FeCl_3$), cobalt nitrate ($CoN_2O_6.6H_2O$), neodymium nitrate [$Nd(NO_3)_3.6H_2O$], nickel(II) acetate [$Ni(CH_3COO)_2.4H_2O$], cerium(III) nitrate [$Ce(NO_3)_3.6H_2O$], chromium(III) nitrate [$Cr(NO_3)_3.9H_2O$] and sodium hydroxide were purchased from Merck Chemical Co.

Synthesis of pure Fe_3O_4, Nd doped Fe_3O_4 and M–Nd doped Fe_3O_4 nanoparticles (M = Co, Ce, Cr, Ni)

To synthesis magnetic nanoparticles the co-precipitation of Fe^{3+} and Fe^{2+} were used with a molar ratio of 2:1. The aqueous solution of sodium hydroxide was used as the precipitating agent. Briefly, to synthesis pure Fe_3O_4 nanoparticles ferrous sulfates heptahydrate (1×10^{-3} mol) and anhydrous ferric chloride (2×10^{-3} mol) were dissolved in 200 mL distilled and deoxygenated water. To synthesis Nd doped Fe_3O_4 nanoparticles, neodymium nitrate (2.5×10^{-3} mmol) and to synthesis M-Nd doped Fe_3O_4 nanoparticles (M = Co, Ce, Cr, Ni), neodymium nitrate (2.5×10^{-3} mmol) and salt of M (3.6×10^{-3} mmol) (salt of M: cobalt nitrate or chromium(III) nitrate or cerium(III) nitrate or nickel(II) acetate) also were added to the 200 mL solution. When the reaction mixture was sonicated, aqueous sodium hydroxide (1.4×10^{-2} mol) was dropped gradually into the mixture solution. It was observed that the solution became black due to the formation of magnetic nanoparticles. Next, the reaction mixture was sonicated and heated up to 80 °C for 30 min. Finally, the magnetic nanoparticles were first washed with distilled and deoxygenated water until the pH value descended to 4.5, and were then kept in -10 °C for 12 hour in n-hexane before production was dried in a vacuum.

Detection method

Fourier transform infrared (FT-IR) spectroscopy was recorded on a Bruker FT-IR. The transmission electron micrographs were obtained with a Zeiss (EM900) transmission electron microscope (TEM) to observe the particle size and morphology. A Bruker-D8ADVANCE X-ray diffractometer revealed X-ray powder diffraction (XRD) pattern when using Cu-Ka radiation (K = 0.15405 nm) to determine the crystal structure of the NPs. The magnetic properties of the composite were measured on a vibrating sampling magnetometer (VSM) 7307 (Lakeshore Co.).A Philips (EL30) was used to obtain a scanning electron microscope analysis (SEM) and an energy dispersive X-ray spectroscopy (EDS).

RESULTS AND DISCUSSION

Size and shape

Using SEM, the shape of Fe_3O_4 magnetic nanoparticles were observed, the results revealed that the magnetic nanoparticles were spherical shaped (Figure 1). The result of EDS images of as-synthesized Nd-M doped Fe_3O_4 nanoparticles and the weight percentage of elements are presented in Table 1. The size and shape of Fe_3O_4 magnetic nanoparticles was observed directly by TEM. The particle size of Fe_3O_4, Nd-Co doped Fe_3O_4 samples measured approximately 15 nm (Figure 2).

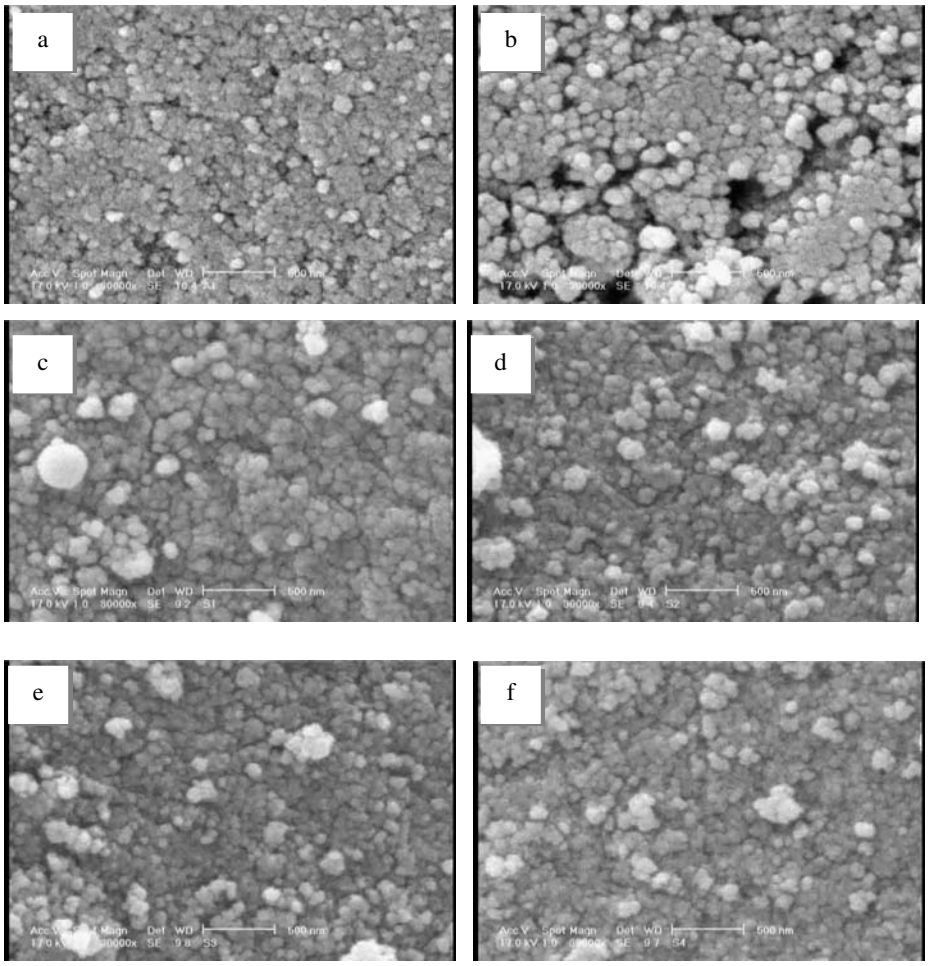

Figure 1. SEM images of (a) Fe_3O_4, (b) Fe_3O_4 doped with Nd^{3+} and Co^{2+}, (c) Fe_3O_4 doped with Nd^{3+}, (d) Fe_3O_4 doped with Nd^{3+} and Ce^{3+}, (e) Fe_3O_4 doped with Nd^{3+} and Cr^{3+}, and (f) Fe_3O_4 doped with Nd^{3+} and Ni^{2+}. The scale bars of images are 500 nm.

Table 1. The weight percentage of elements.

Nd-M doped Fe_3O_4	Fe wt%	Nd wt%	M wt%
Nd doped Fe_3O_4	98.36	1.64	-
Nd-Co doped Fe_3O_4	97.81	0.81	1.38
Nd-Ce doped Fe_3O_4	95.81	2.19	1.99
Nd-Cr doped Fe_3O_4	97.39	1.82	0.8
Nd-Ni doped Fe_3O_4	96.44	1.66	1.90

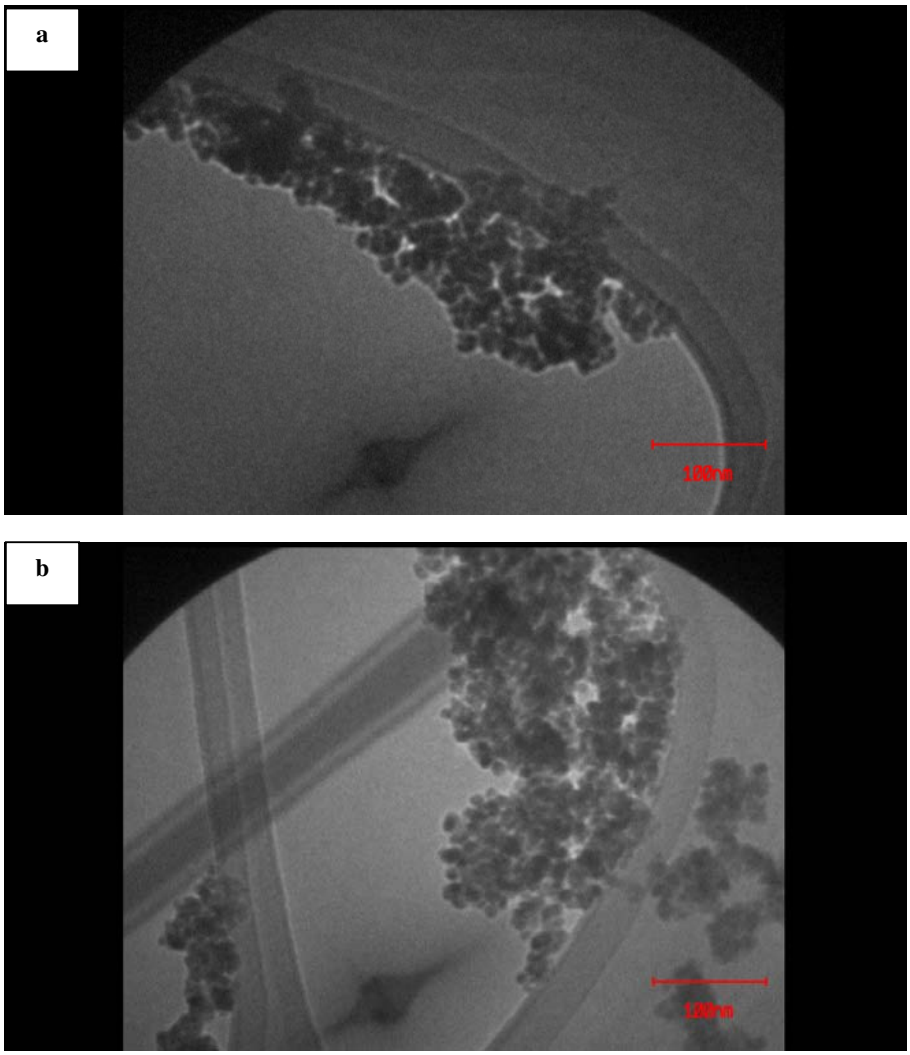

Figure 2. TEM micrographs of (a) magnetite and (b) Fe_3O_4 doped with Nd^{+3} and Co^{+2}. The scale bars of images are 100 nm.

Structure of crystal

Figure 3 shows the XRD patterns of Fe_3O_4, Co-Nd doped Fe_3O_4, Nd doped Fe_3O_4, Nd-Ce doped Fe_3O_4, Nd-Cr doped Fe_3O_4 and Nd-Ni doped Fe_3O_4 nanoparticles. Table 2 compare the angles of peaks appeared in XRD patterns of synthesized samples with angles of XRD pattern and crystal plane of spinel ferrite. Results showed the peaks appeared at 2Θ in XRD patterns of synthesized samples were well indexed to the angles and crystal plane of spinel ferrite.

The average crystallite diameter (D) of the 15 nm Fe_3O_4 nanoparticles was calculated from the strongest peak based on the Debye-Scherrer formula [30].

$$D = \frac{0.89\lambda}{\beta\cos\theta},$$

where λ is the X-ray wavelength, θ the angle of Bragg diffraction and β the difference between FWHM and the instrumental broadening. The determined D was calculated to be about 9.14 nm, which was in agreement with TEM results as shown in Figure 2a.

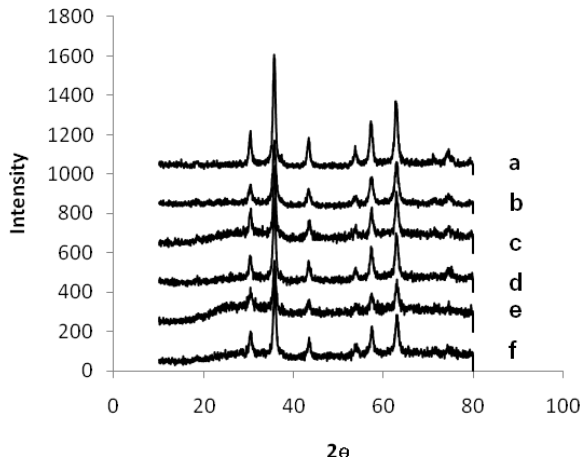

Figure 3. XRD patterns of (a) Fe_3O_4, (b) Fe_3O_4 doped with Nd^{3+} and Co^{2+} (c) Fe_3O_4 doped with Nd^{3+}, (d) Fe_3O_4 doped with Nd^{3+} and Ce^{3+}, (e) Fe_3O_4 doped with Nd^{3+} and Cr^{3+}, and (f) Fe_3O_4 doped with Nd^{3+} and Ni^{2+}.

Table 2. The angles of XRD pattern and crystal plane of spinel ferrite compare with the angles of XRD patterns of synthesized samples.

Spinel ferrite (hkl)	(111)	(220)	(311)	(400)	(422)	(511)	(440)	(620)	(533)
Spinel ferrite (2θ)	18.28	30.10	35.45	43.12	53.48	57.01	62.59	70.97	74.06
Fe_3O_4 (2θ)	18.37	30.11	35.46	43.09	53.38	56.97	62.64	70.95	74.28
Nd doped Fe_3O_4 (2θ)	18.41	30.46	35.77	43.38	53.79	57.40	63.03	71.60	74.51
Co-Nd doped Fe_3O_4 (2θ)	-	30.02	35.60	43.26	-	57.20	62.70	-	-
Nd-Ce doped Fe_3O_4 (2θ)	18.62	30.34	35.71	43.38	53.85	57.36	62.95	71.68	-
Nd-Cr doped Fe_3O_4 (2θ)	18.36	30.23	35.72	43.32	53.77	57.32	62.81	71.47	74.32
Nd-Ni doped Fe_3O_4 (2θ)	18.49	30.45	35.62	43.47	53.86	57.47	62.89	71.31	74.78

Magnetic properties

Figure 4 shows the Magnetization loops of Fe_3O_4 and Nd-Co doped Fe_3O_4, Nd doped Fe_3O_4,Nd-Cr doped Fe_3O_4 and Nd-Ce doped Fe_3O_4 and Nd-Ni doped Fe_3O_4 NPs. Magnetic properties of NPs were characterized by vibrating sampling magnetometer (VSM). It can be seen that no coercivity or remanence could be observed with all three samples, suggesting the presence of superparamagnetic properties of the Fe_3O_4 NPs. This can be ascribed to the small size of NPs which were smaller than the superparamagnetic critical size (25 nm). The saturation magnetization (M_s) of Fe_3O_4, Fe_3O_4 doped with Nd^{3+}, Fe_3O_4 doped with Nd^{3+}-Co^{2+}, Fe_3O_4 doped with Nd^{3+}-Ce^{3+}, Fe_3O_4 doped with Nd^{3+}- Cr^{3+} and Fe_3O_4 doped with Nd^{3+}- Ni^{2+} NPs were 56.66,

40.72, 74.64, 48.98, 40.14, 44.85 emu.g^{-1}. Apparently, synthesized Fe_3O_4 nanoparticles had relatively lower magnetic values than that of bulk Fe_3O_4 (93 emu.g^{-1}). It is well-known that magnetic property of particles is size-dependent. For relatively larger particles, magnetic domains were formed to reduce the static magnetic energy. The number of domains diminished with decreasing particle size. The particles turned into single domain ones at a low size, resulting in the decrease of saturation magnetization due to vanishing of the magnetization caused by the movement of domain walls. A single-domain state existed when the size of a particle was below the critical diameter (Dc) of a spherical particle. Typical value of Dc for Fe_3O_4 was 128 nm [31] which were much larger than 15 nm.

Magnetite has inverse spinel structure of the type $Fe^{2+}Fe_2^{3+}O_4$, in this cubic inverse spinel structure, oxygen forms a FCC closed packing and half of Fe^{3+} cations occupying the interstitial tetrahedral sites, half of them occupying the octahedral sites and Fe^{2+} cations occupying the rest of the octahedral sites [2]. According to the structure of inverse spinel in external magnetic field, orientation of magnetic moments of Fe^{3+} cations in octahedral and tetrahedral sites are against each other and neutralize the magnetic properties of Fe^{3+} cations. So Fe^{2+} cations is responsible for the magnetic property of magnetite. The saturation magnetization of Fe_3O_4 doped with Nd, Nd-Ce, Nd-Cr and Nd-Ni NPs were lower than the pristine Fe_3O_4 NPs. This reduction can be caused by Nd, Ce, Cr, Ni substitutions with Fe^{2+} cations. It was found that the magnetic response of the Fe_3O_4 increased when it was doped with Nd^{+3} and Co $^{+2}$. The improvement of saturation magnetization in pure spinel ferrite Fe_3O_4 can be caused by Co substitutions with Fe^{3+} cations. Ishikawa *et al.* [32] reported that the Fe_3O_4 particles doped with Co^{2+} exhibited high Fe^{2+} contents, as mentioned before high Fe^{2+} contents in magnetite structure results high magnetic properties. The high saturation magnetization indicated excellent crystal structure. Nanoparticles were characterized in 10000 Oe applied field.

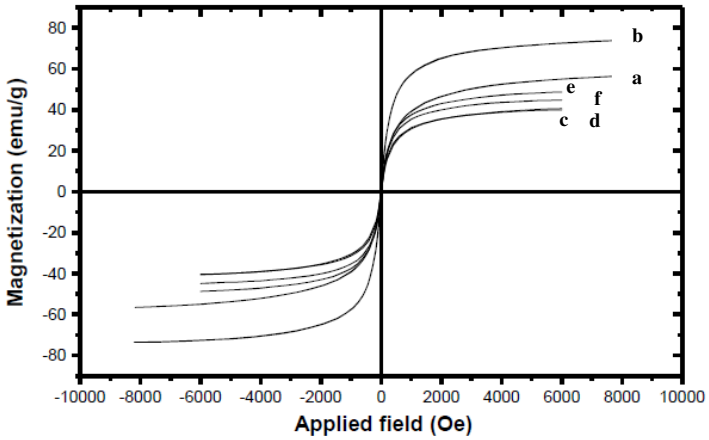

Figure 4. Field-dependent magnetization of (a) Fe_3O_4, (b)Fe_3O_4 doped with Nd^{3+} and Co^{2+}, (c) Fe_3O_4 doped with Nd^{3+}, (d) Fe_3O_4 doped with Nd^{3+} and Cr^{3+}, (e) Fe_3O_4 doped with Nd^{3+} and Ce^{3+} (f) Fe_3O_4 doped with Nd^{3+} and Ni^{2+}.

FT-IR analysis

Figure 5 shows FT-IR spectrum of the magnetic nanoparticles obtained. The FT-IR spectrum of iron oxide exhibits strong bands in the low-frequency region (1000–500 cm^{-1}) due to the iron

oxide skeleton, which is consistent with the magnetite (Fe_3O_4) spectrum. For Fe_3O_4, two major bands at 583 and 424 cm^{-1} are ascribed to Fe–O stretching modes of tetrahedral and octahedral sites in magnetite, respectively [33, 34]. The peak at 3439 cm^{-1} was the characteristic of stretching vibration of OH. It can be deduced that $Fe(OH)_2$, $Fe(OH)_3$ and FeOOH formed resulting from hydrolyzation on the surface of Fe_3O_4. While the peak at 1633 cm^{-1} also shows existence of Fe–O. The shift of the band at 583 and 424 cm^{-1} should be ascribed to the change in the bonding force between the cations and the oxygen anion arising from the presence of Nd, Co, Ce, Cr and Ni, which presents a stronger or weaker ionic bond [35]. This indicates that dopant cations are occupied in both octahedral and tetrahedral sites.

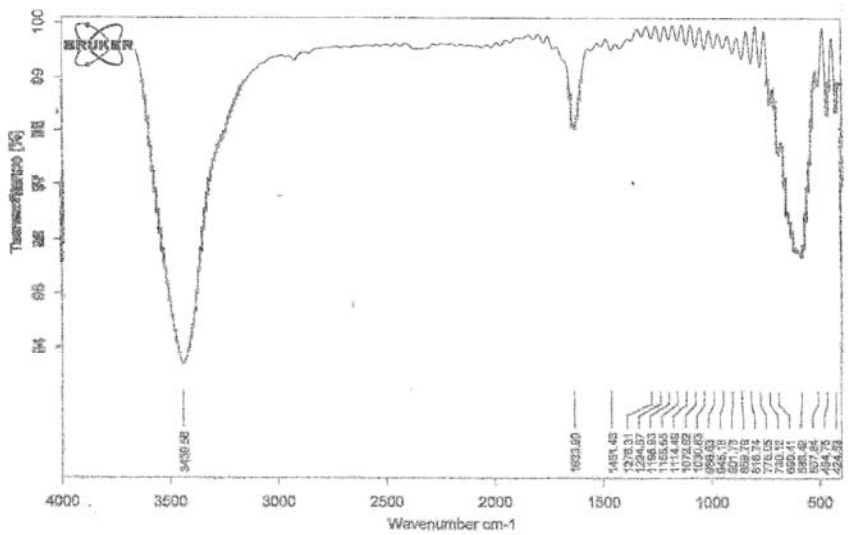

Figure 5. FTIR spectra of synthesized magnetic nano particles.

CONCLUSIONS

In this paper, the magnetic NPs were prepared by the co-precipitation method. The results revealed that the as-synthesized NPs were spherical shaped with inverse spinel structure. The particle size of the magnetic NPs was approximately 15 nm. Magnetic measurements revealed that the magnetic NPs exhibited superparamagnetic property; the Nd–Co doped Fe_3O_4 nanoparticles had a better magnetic property than the pristine Fe_3O_4 NPs. The saturation magnetization of the Nd-Co doped Fe_3O_4 NPs was 74.64 $emu.g^{-1}$. The saturation magnetization of Nd doped Fe_3O_4 , Nd-Ce doped Fe_3O_4, Nd-Cr doped Fe_3O and Nd-Ni doped Fe_3O_4 NPs was lower than the pristine Fe_3O_4 NPs, which were 40.72, 48.98, 40.14, 44.85 $emu.g^{-1}$, respectively. The as-synthesized magnetic NPs nanoparticles are expected to be applied in magnetic and biomedicine fields.

ACKNOWLEDGEMENTS

This work was financially supported by Iranian Nano Technology Initiative Council. The support by the Islamic Azad University Shahr-e-Rey Branch is acknowledged.

REFERENCES

1. Frey, N.; Peng, S.; Cheng, K.; Sun, *S. Chem. Soc. Rev*. **2009**, 38, 2532.
2. Verwey, E. *Nature* **1939**, 144, 327.
3. Nayar, S.; Mir, A.; Ashok, A.; Sharma, A. *J. Bionic Eng*. **2010**, 7, 29.
4. Moodley, P.; Scheijen, F.; Niemantsverdriet , J.; Thüne, P. *Catal. Today* **2010**, 154, 142.
5. Haw, C.; Mohamed, F.; Chia, C.; Radiman, S.; Zakaria, S.; Huang, N.; Lim, H. *Ceram. Int.* **2010**, 36, 1417.
6. Yang, X.; Chen, L.; Han, B.; Yang, X.; Duan, H. *Polymer* **2010**, 51, 2533.
7. Kempe, H.; Kempe, M. *Biomaterials* **2010**, 31, 9499.
8. Li, Z.; Kawashita, M.; Araki, N.; Mitsumori, M.; Hiraoka, M.; Doi, M. *Mater. Sci. Eng.* **2010**, 30, 990.
9. Luo, H.; Wang, D.; He, J.; Lu, Y. *J. Phys. Chem. B* **2005**, 109, 1919.
10. Pelecky, D.L.L.; Rieke, R.D. *Chem. Mater*. **1996**, 8, 1770.
11. Ko, S.W.; Yang, M.S.; Choi, H.J. *Mater. Lett*. **2009**, 63, 861.
12. Park, B.J; Fang, F.F.; Choi, H.J. *Soft Matter*. **2010**, 6, 5246.
13. Xiao, H.M.; Liu, X.M.; Fu, S.Y. Compos. *Sci. Technol*. 2006, 66, 2003.
14. Wang, X.; Zhuang, J.; Peng, Q.; Li, Y. *Nature* **2005**, 437, 121.
15. Deng, H.; Li, X.; Peng, Q.; Wang, X.; Chen, J.; Li, Y. *Angew. Chem. Int. Ed.* **2005**, 44, 2782.
16. Zhao, D.; Wu, X.; Guan, H.; Han, E. *J. Supercrit. Fluid* **2007**, 42, 226.
17. Feng, J.; Guo, L.Q.; Xu, X.; Qi, S.Y.; Zhang, M.L. *Physica*. B **2007**, 394, 100.
18. Xuan, Y.; Li, Q.; Yang, G. *J. Magn. Magn. Mater*. **2007**, 312, 464.
19. Cheng, Y.; Zheng, Y.; Wang, Y.; Bao, F.; Qin, Y. *J. Solid State Chem*. **2005**, 178, 2394.
20. Bee, A.; Massart, R.; Neveu, S. *J. Magn. Magn. Mater*. **1995**, 149, 6.
21. Cushing, B.L.; Kolesnichenko, V.L.; O'Connor, C. *J. Chem. Rev*. **2004**, 104, 3893.
22. Willis, A.L.; Turro, N.J.; O'Brien, S. *Chem. Mater*. **2005**, 17, 5970.
23. Christoskova, S.G.; Stoyanova, M.; Georgieva, M. *Appl. Catal. A-Gen*. **2001**, 208, 235.
24. Area´n, C.O.; Mentruit, M.P.; Platero, E.E.; Xamena, F.X.L.; Parra, J.B. *Mater. Lett.* **1999**, 39, 22.
25. Liu, C.; Zou, B.; Rondinone, A.J.; Zhang, J.Z. *J. Phys. Chem. B* **2000**, 104, 1141.
26. Woo, K.; Lee, H.J.; Ahn, J.P.; Park, Y.S. *Adv. Mater*. **2003**, 15, 1761.
27. Ge, J.P.; Chen, W.; Liu, L.P.; Li, Y.D. *Chem. Eur. J.* **2006**, 12, 6552.
28. Moumen, N.; Veillet, P.; Pileni, M.P. *J. Magn. Magn. Mater.* **1995**, 149, 67.
29. Kommareddi, N.S.; Tata, M.; John, V.T.; McPherson, G.L.; Herman, M.F.; Lee, Y.S.; O'Connor, C.J.; Akkara, J.A.; Kaplan, D. *Chem. Mater*. **1996**, 8, 801.
30. Mandal, K.; Mandal, S.P.; Agudo, P.; Pal, M. *Appl. Surf. Sci*. **2002**, 182, 386.
31. Kittel, C. *Phys. Rev*. **1946**, 70, 965.
32. Ishikawa, T.; Nakazaki, H.; Yasukawa, A.; Kanddori, K.; Sato, M. *Corrosion Sci*. **1999**, 41, 1665.
33. Mandal, M.; Kundu, S.; Ghosh, S.K.; Panigrahi, S.; Sau, T.K.; Yusuf, S.M.; Pal, T. *J. Colloid Interface Sci*. **2005**, 286, 187.
34. Gnanaprakash, G.; Philip, J.; Jayakumar, T.; Raj, B. *J. Phys. Chem. B* **2007**, 111, 7978.
35. Nohair, M.; Aymes, D.; Perriat, P.; Gillot, B. *Vib. Spectrosc*. **1995**, 9, 181.